O. Kostyuk[1,2], B. Dzundza[1], M. Maksymuk[3], V. Bublik[4], L. Chernyak[5], Z. Dashevsky[6]

Development of Spark Plasma Sintering (SPS) for preparation of nanocrystalline *p*-type Bi0.5Sb1.5Te3 thermoelectric material

[1]*Vasyl Stefanyk Precarpathian National University, Ivano-Frankivsk, Ukraine, bdzundza@gmail.com*
[2]*Ivano-Frankivsk National Medical University, Ivano-Frankivsk, Ukrain, oksanakostuk@gmail.com*
[3]*Faculty of Materials Science and Ceramics, AGH University of Science and Technology, Krakow, Poland*
[4]*Moscow Institute of Steel and Alloys, National University of Science and Technology, Moscow Russia, bublik_vt@rambler.ru*
[5]*University of Central Florida, USA, Leonid.Chernyak@ucf.edu*
[6]*Ben-Gurion University of the Negev, Beer-Sheva, Israel, dashevsky.45@mail.ru*

Bismuth antimony telluride is the most commonly used commercial thermoelectric material for power generation and refrigeration over the temperature range of 200 - 400 K. Improving the performance of these materials is complected balance of optimizing thermoelectric properties. Decreasing the grain size of Bi0.5Sb1.5Te3 significantly reduces the thermal conductivity due to the scattering phonons on the grain boundaries. In this work, it is shown the advances of spark plasma sintering (SPS) for preparation of nanocrystalline *p*-type thermoelctrics based on Bi0.5Sb1.5Te3 at different temperatures (240, 350, 400ºC). The complex study of structural and thermoelectric properties of Bi0.5Sb1.5Te3 were presented. The high dimensionless thermoelectric figure of merit *ZT* ~ 1 or some more over 300 - 400 K temperature range for nanocrystalline *p*-type Bi0.5Sb1.5Te3 was obtained.

Key words: Bi0.5Sb1.5Te3**,** Spark plasma sintering (SPS), thermoelectric properties, figure of merit *Z*.

Received 10 November 2020; Accepted 15 December 2020.

Introduction

Choice criteria of effective thermoelectric material was stated by A.F. Ioffe as "*The material with the electrical conductivity like a good metal and the thermal conductivity like good isolator*". A.F. Ioffe deserves a full credit for understanding that namely "middle" class of materials – semiconductors can provide the best thermoelectric performance as thermoelectric materials [1]. The conversion efficiency of heatenergy to electric power depends on figure of merit of thermoelectric material – factor *Z*, which his expressed as:

$$Z = \frac{S^2 \sigma}{\kappa},\qquad(1)$$

where *S* is Seebeck coefficient, σ is electrical conductivity and *κ* is thermal conductivity of thermoelectric material.

At acoustic phonon scattering of charge carriers (charge carriers mean free path $l = l_0 E^r$, where l_0 is constant, *E* is charge carrier energy, scattering parameter

r = 0), Seebeck coefficient is written as:

$$S = \frac{k_0}{e}\left[2\frac{F_1\left(\mu^*\right)}{F_0\left(\mu^*\right)} - \mu^* \right],\qquad(2)$$

where k_0 is Boltzmann constant, *e* is electron charge, F_i are Fermi integrals, μ* is reduced Fermi level (for conduction band μ* = $(E_c - E_F)/k_0 T$, E_c is the bottom of conduction band, E_F is Fermi level, for valence band μ* = $(E_F - E_V)/k_0 T$, E_v is the top of valence band).

The electrical conductivity σ of a semiconductor with density of charge carriers *n(p)* is given by well-known formula:

$$\sigma = en(p)\mu_n(\mu_p),\qquad(3)$$

where *n(p)* is electron (hole) concentration, $\mu_n(\mu_p)$ is mobility of charge carriers.

The hole concentrations in the valence band is:

$$p = 4\pi \frac{\left(2m_p^* k_0 T\right)^{\frac{3}{2}}}{h^3} F_{1/2}\left(\mu^*\right),\qquad(4)$$

where m^*_p is the density of state effective (DOS) mass of holes. The mobility in a semiconductor with a simple parabolic band is written as:

$$\mu = e\tau / m^*_c, \qquad (5)$$

where τ is the average pulse relaxation time (the time defining a mean free path), and m^*_c is effective mass of charge carrier.

Heat transport is determined by total thermal conductivity κ of semiconductor which consists of three components: lattice thermal conductivity κ_L by phonons, electronic thermal conductivity κ_e by free electrons or holes and ambipolar thermal conductivity κ_a by electron - hole pairs in the intrinsic conduction region:

$$\kappa = \kappa_L + \kappa_e + \kappa_a. \qquad (6)$$

The heat transport by any elementary excitations (phonons) can be described by formula:

$$\kappa_L = \frac{1}{3} C_v v^3, \qquad (7)$$

where C_v is the specific heat at constant volume, v is the velocity of propagation of an elementary excitation. Electronic thermal conductivity can be described by Wiedemann - Franz law:

$$\kappa_e = L_0 \sigma T \qquad (8)$$

where L_0 is constant known as Lorenz number. For scattering by the acoustic phonons, Lorenz number is given by:

$$L_0 = 2\left(\frac{k_0}{e}\right)^2. \qquad (9)$$

Seebeck coefficient S decreases with a growth of charge carriers concentration $n(p)$ and in a metal with charge carriers concentration~ 10^{22} cm^{-3} S close to zero. At the same time, electrical conductivity σ increases with growth of charge carriers concentration $n(p)$. Therefore, dependence of product $S^2\sigma$ as a function of Fermi level E_F has the bell-shaped form. The maximum $S^2\sigma$ is achieved, when E_F is close to the bottom of conduction band in n-type semiconductor or close to the top of valence band for p-type semiconductor. In this case value of Seebeck coefficient $S \approx 180 \pm 10\mu V/K$ and charge carriers concentration $n(p) \sim 5 \times 10^{19}$ cm^{-3}. When charge carriers concentration $n(p) \sim 5 \times 10^{19}$ cm^{-3}, then heat transport is determined mainly by lattice thermal conductivity κ_L by phonons. For the optimal charge carrier concentration (reduced Fermi level $\mu^* \approx 0$), figure of merit Z practically depends on three parameters:

$$Z \sim m_n^{*3/2}(\mu / \kappa_L). \qquad (10)$$

Now we can formulate the choice criteria of the effective thermoelectric material:

1. Semiconductor material (elemental, compound, alloy, composite, multilayer, superlattice, low-dimension) should preferably consists of heavy atoms that will cause a low frequency of thermal vibrations of lattice and, correspondingly, significant decrease in lattice thermal conductivity κ_L.

2. Semiconductor material should have high dielectric constant $\varepsilon \geq 100$, that reduces significantly the scattering of charge carriers by impurity ions; and small effective mass of major charge carriers. These two requirements provide high mobility of charge carriers μ. Note, that high dielectric constant ε leads to decrease in ionization energy of the impurity atoms (which practically approaching zero). As a result, energy level of impurity merges with the valence band, and concentration of holes in the valence band in p-type becomes constant (like a metal) and equals to concentration of dopant from 0 K to the onset of intrinsic conductivity.

3. Semiconductor material should have multi-valley structure (equivalent ellipsoids) of the valence band. This leads to an increase in concentration of charge carriers and, correspondingly, the electrical conductivity σ, which is proportional to the number of ellipsoids, without changing energy of Fermi level E_F.

4. Impurity doping of semiconductor material to the level $p \geq 10^{19}$ cm^{-3} should be possible that will provide optimal Fermi level energy E_F, and, having in mind maximum value of $S^2\sigma$, will mean $(E_v - E_F) \sim 0$ eV.

5. Band gap of semiconductor over operating temperature range of thermoelectric material should be not less than $E_g \geq 8 k_0 T$ to minimize contribution of thermally generated minority charge carriers to total electrical conductivity leading to decrease in thermoelectric efficiency.

6. Creation of binary solid solutions with a goal of increasing the ratio of carrier mobility to lattice conductivity (A.F. Ioffe idea).

7. Good mechanical properties [2-3].

Alloys of Bi_2Te_3 and Sb_2Te_3 are the best performing p-type thermoelectrics near room temperature and have been the subject of extensive engineering efforts [4-10]. The main properties of p-type thermoelectric material on $(BiSb)_2Te_3$ semiconductor alloys are presented in Table 1. Bi_2Te_3 based compounds have defect structure [11]. Thermodynamic nature of defect systems in chalcogenide materials are decribed such carefully in [12, 13].

In the last years interest in low dimensional thermoelectric structures has increased due to the possibility of sharply increasing their figire of merit Z [14, 15]. The first effect of a significant increase in Z were observed in quantum wells of the thermoelctric materials. However such structures with dimensions in order some μm can not be used for fabrication of the thermolectric devices in different real applications. Therefore researchers have turned their attention to the creation of bulk and film nanostructured thermoelectrics [16-19].

The spark plasma sintering (SPS) technology was used after the nanopowder fabrication in the high energy ball mill. SPS is a new method of sintering under pressure with the pulse direct current transmission. This metod allows to sinter specimens at relatively low temperatures during a short time. SPS syntering restricticts the undesirable growth of grains due to recrystallization process.

O. Kostyuk, B. Dzundza, M. Maksymuk, V. Bublik, L. Chernyak, Z. Dashevsky

Table 1

The main properties of *p*-type thermoelectric material on $(BiSb)_2Te_3$ semiconductor alloys

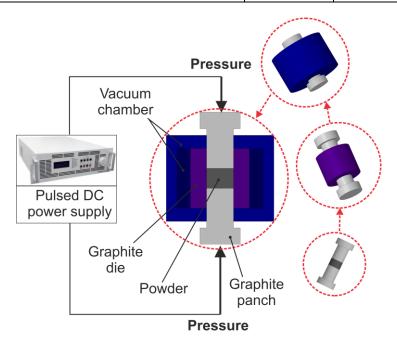| Composition	Parameter	Symbol	Value	Reference
Bi_2Te_3	Melting point	T_m	858 K	[4]
Bi_2Te_3	Band-gap at 300 K	Eg	0.13 eV	[4]
Bi_2Te_3	Temperature dependence of band-gap	dE_g/dT	-9×10^{-5} eV/K	[4]
Bi_2Te_3	Debye temperature	T_D	155.5 K	[4]
Bi_2Te_3	Number of ellipsoids at valence band	N_v	6	[4]
Bi_2Te_3	Density of states effective mass of holes	m^*_p	$0.69 m_o$	[4]
Bi_2Te_3	Hole mobility at $T = 300$ K	μ_p	510 cm^2/Vs	[4]
Bi_2Te_3	Scattering parameter	r_p	0	[4]
Bi_2Te_3	Dielectric constant	ε_o	400	[4]
Bi_2Te_3	Intrinsic carrier concentration at $T = 300$ K	n_i	10^{18} cm^{-3}	[4]
Bi_2Te_3	Lattice thermal conductivity at $T = 300$ K	κ_L	1.4 W/mK	[4]
$Bi_{0.5}Sb_{1.5}Te_3$	Lattice thermal conductivity at $T = 300$ K	κ_L	1.0 W/mK	[5]
Bi_2Te_3	Dimensionless Figure of Merit at $T = 300$ K	ZT	0.8	[4]
$Bi_{0.5}Sb_{1.5}Te_3$	Dimensionless Figure of Merit at $T = 300$ K	ZT	1.1	[5, 6]

Fig. 1. Schematic view of SPS technique set up.

I. Experimental procedure

Synthesis of materials was carried out in quartz ampoules evacuated to a residual pressure of 10^{-4} mbar. The ampoules were subjected to detailed purification, which included washing in $HNO_3:H_2SO_4$ mixture and frequent cleaning with distilled water and isopropanol. Polycrystalline samples $Bi_{0.5}Sb_{1.5}Te_3$ were synthesized by melting the elements Bi (Alfa Aesar, 99.999 %), Te (Alfa Aesar, 99.999 %) and Sb (Alfa Aesar, 99.99 %) at 750 ºC in a rocking furnace that can vary the angle in the range of ± 30º with a period of 15 s to force mixing the

components. At temperature~ 900 ºC the ampoule was taken from the furnace and quenched in cold water. The ingots were subjected to mechanical activation in a protective atmosphere in AGO-2U high energy planetary ball mill.

After that the nanopowder was compacted in a protective atmosphere at room temperature into tablets into a 20-mm diameter and 5-mm thickness under pressure of 1 GPa. Then, these tablets were densified by Spark Plasma Sintering (SPS) method, which was first developed by Prof. Z. Dashevsky for Bi_2Te_3 and PbTe thermoelectrics [19-21]. The schematic view of SPS technique set is presented in Fig. 1. The temperature of sintering was at 400ºC during 20 min under an axial
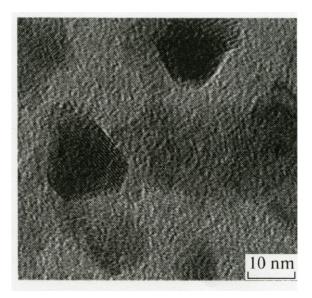
Fig. 2. Electron microscope image of $Bi_{0.5}Sb_{1.5}Te_3$ powder particles.

compressive stress of 60 MPa in an argon atmosphere. The heating/cooling rate was 50 °C/min.

Phase identification was performed with the Bruker D8 advance X-ray diffractometer using $Cu_{K\alpha1}$ radiation ($\alpha = 1.5406$ Å, $\Delta 2\Theta = 0.005°$, 2Θ range 10 - 120°) with Bragg-Brentano geometry. Lattice parameters refinement and other crystallographic calculations were performed with the program package GSAS-II. For SEM and EDX analyses, samples were embedded in conductive resin, and subsequently polished, finally using 1 μm diamond powder in a slurry. The analysis of the samples chemical composition was performed using scanning electron microscopy (JEOL JSM-6460LV Scanning Electron Microscope) equipped with energy dispersive X-ray spectroscopy. The uniformity of the Seebeck coefficient at sample surface (10 mm x 2.2 mm) was performed by the scanning thermoelectric microprobe (STM) technique with 50 μm resolution.

The Seebeck coefficient S and electrical conductivity σ were measured by commercial apparatus SBA 458 Nemesis developed by Netzsch. Measurements were spent in argon at the temperature range from 25 to 500 °C. Thermal diffusivity α was measured by the Netzsch LFA 457 equipment and the specific heat capacity C_p was derived from a reference sample (Pyroceram 9606). The samples were firstly spray coated with a thin layer of graphite to minimize errors from the emissivity of the material and from laser beam reflection caused by shiny pallet surface. Thermal conductivity was calculated using the equation:

$$\kappa = \alpha \rho c_p, \qquad (11)$$

where ρ is the density obtained by Archimedes principle at the discs from PECS. The uncertainty of the Seebeck coefficient and electrical conductivity measurements is 6 %, the uncertainty of the thermal conductivity is estimated to be within 8%. The combined uncertainty for the experimental determination of ZT is ~ 20 %.

II. Results and discussion

2.1. The structure of $Bi_{0.5}Sb_{1.5}Te_3$ powder

It was observed by the transmission electron microscopy powder particles preserved $Bi_{0.5}Sb_{1.5}Te_3$ composition have good structure perfection. The average size of powder particles, determined from high resolution transmission microscopy ~ 10 - 12 nm (Figure 2).

2.2. The structure of $Bi_{0.5}Sb_{1.5}Te_3$ specimens prepared by SPS method

The specimens, compacted from nanopwders at room temperature, after Spark Plasma Sintering, were mechanically strong at the sintering temperatures. Pores were absent. The cleavage surface images, were inverstigated in the scanning electron microscope, are presented in Fig. 3. The crystallites growth is observed at 350 - 400°C temperature range. In the remaining samples the structure is finely dispersed. Thus, mechanical milling consequences are preserved, and, at temperatures of 350°C and higher, particles grow, pointing to the active recrystallization process.

2.3 Thermoelectric properties

Seebeck coefficient (a) electrical conductivity (b), thermal conductivity (c) and calculated a dimensionless figure of merit ZT (d) have been measured in the temperature range of 200 - 400 K for specimens, prepared by the SPS at different temperatures (240, 350, 400°C).

The lattice thermal conductivity κ_L was determined by subtracting the electronic thermal conductivity κ_e from the total thermal conductivity κ (Figure 4(c)). The values of κ_e were calculated using Wiedemann-Franz law (Eq. 8). The Lorentz number L, which was calculated using the following equation [5]:

$$L = \left(\frac{k_0}{e}\right)^2 \left[3\frac{F_2(\mu^*)}{F_0(\mu^*)} - \left(2\frac{F_2(\mu^*)}{F_0(\mu^*)}\right)^2\right], \qquad (12)$$

where k_0 is Boltzmann constant, e is the electron charge, $\mu^* = E_F/k_0T$ is the reduced Fermi energy, and $F_x(\mu^*)$ is the Fermi integral given by:

$$F_x(\mu^*) = \int_0^\infty \frac{E^x dE}{1 + \exp(E - \mu^*)}. \qquad (13)$$

At acoustic phonon scattering of electrons, the reduced Fermi energy μ^* can be obtained from fitting the Seebeck coefficient [5]:

$$S = \frac{k_0}{e}\left[\frac{2F_1(\mu^*)}{F_0(\mu^*)} - \mu^*\right]. \qquad (14)$$

Values of the lattice thermal conductivity κ_L at 300 K for specimens prepared by SPS at 350 - 400°C ≈ 0.8 W/m K. This value of κ_L for specimens with nanocrystlline structure on ~ 30 % less than κ_L for best $Bi_{0.5}Sb_{1.5}Te_n_xTe_3$ polycrystals prepared by hot extrusion [5]. A significant decrease in the value of κ_l may be due to the scattering of long wave phonons on the grain boundaries [22, 23].

It is shown the high value of ZT on a level ≈ 1 and some more over 300 - 400 K temperature range for nanocrystalline $Bi_{0.5}Sb_{1.5}Te_n_xTe_3$ specimens prepared

O. Kostyuk, B. Dzundza, M. Maksymuk, V. Bublik, L. Chernyak, Z. Dashevsky
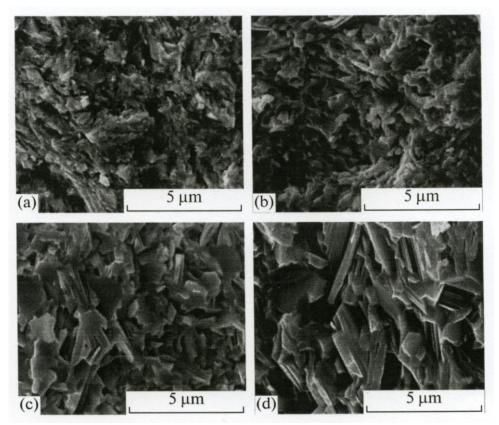
Fig. 3. Secondary emission images of specimens, prepared by the SPS at temperatures of (a) 240, (b) 300, (c) 350, and (d) 400°C.
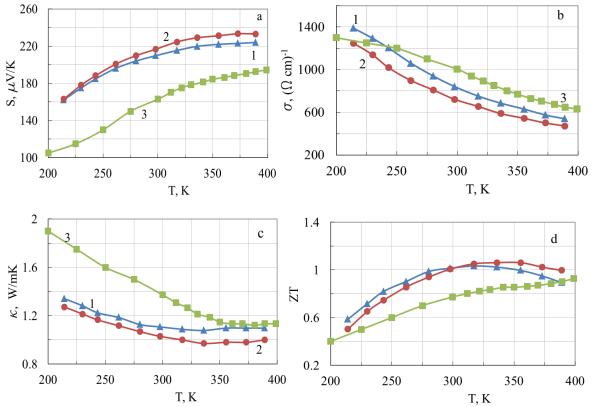

Fig. 4. Seebeck coefficient (a), electrical conductivity (b), thermal conductivity (c) and dimensionless figure of merit ZT (d) as a function of temperature for $Bi_{0.5}Sb_{1.5}Te_{n}x Te_3$ specimens prepared by SPS at different temperatures. 1 - 400, 2 - 350, 3 - 240ºC respectively.

by SPS at 350 - 400ºC temperatures (Fig. 4d).

Conclusions

Spark plasma sintering (SPS) under pressure with the pulse direct current transmission was used for preparation of nanocrystalline *p*-type $Bi_{0.5}Sb_{1.5}Te_3$ thermoelectric material.

Based on structure studies, at the syntering temperatures of 350 °C and higher recrystallization process was observed. It is resulting in increasing of the grain size of the thermoelectric material.

The thermoelectric properties, such as the electrical and thermal conductivities, Seebeck coefficient, for specimens $Bi_{0.5}Sb_{1.5}Te_3$, prepared by the SPS at different temperatures (240, 350, 400 ºC) has been investigated over 200 – 400 K temperature range. The high value of $ZT \approx 1.1$ over 300 - 400 K temperature range for nanocrystalline *p*-type $Bi_{0.5}Sb_{1.5}Te_3$ specimens was obtained. It should be noted, that for specimens prepared by SPS at 350 - 400ºC the significant decrease in the value of κ_L is observed, which may be explained by scattering of long wave phonons on the grain boundaries.

Kostyuk O. – PhD, Senior Researcher;
Dzundza B. – PhD, Associate Professor;
Maksymuk M. – PhD student;
Bublik V. – Professor, Doctor of Sciences;
Chernyak L. – Professor, Doctor of Sciences;
Dashevsky Z. – Professor, Doctor of Sciences.

[1] A.F. Ioffe, B.Ya. Moizes, L.S. Stilbans, Sov. State Physics 11, 2834 (1960).

[2] M.G. Lavrentev, V.B. Osvensky, H.S. Kim, I.T. Witting, G.J. Snyder, V.T. Bublok, Appl. Mat. 4, 104807 (2016) (https://doi.org/10.1063/1.4953173).

[3] Y. Gelbstein, Z. Dashevsky, M.P. Dariel, J. Appl. Phys. 104, 33 (2008) (https://doi.org/10.1063/1.2963359).

[4] I.T. Witting, J.A. Grovogui, V.P. Dravid, G.J. Snyder, J. of Materiomics 6, 532 (2020) (https://doi.org/10.1016/j.jmat.2020.04.001).

[5] Z. Dashevsky, S. Skipidarov, Investigating the performance of bismuth– antimony telluride, in Novel Materials and Deice Design Concepts. Thermoelectric power generation, edited by S. Skipidarov, M. Nikitin (Springer, New York, 2019).

[6] B. Poudel, Q. Hao, Y. Ma, X.Y. Lan, A. Minnich, B. Yu, X. Yan, D.Z. Wang, A. Muto, D. Vashaee, X.Y. Chen, J.M. Liu, M.S. Dresselhaus, G. Chen, and Z.F. Ren, Science 320, 6342 (2008) (https://doi.org/10.1126/science.1156446).

[7] O. Ben-Yehuda, R. Shuker, Y. Gelbstein, Z. Dashevsky, M.P. Dariel, J. of Appl. Phys. 101, 25 (2007) (https://doi.org/10.1063/1.2743816).

[8] O. Ben-Yehuda, Y. Gelbstein, Z. Dashevsky, M.P. Dariel, Proceedings ICT 2007. Jeju. 82 (2007) (https://doi.org/10.1109/ICT.2007.4569429).

[9] Yu Pan, Umut Aydemir, Jann A. Grovogui, Ian T. Witting, Riley Hanus, Yaobin Xu, Jinsong Wu, Chao-Feng Wu, Fu-Hua Sun, Hua-Lu Zhuang, Jin-Feng Dong, Jing-Feng Li, Vinayak P. Dravid, G. Jeffrey Snyder, Adv. Mater. 2018. 1802016, 1 (2018) (https://doi.org/10.1002/adma.201802016).

[10] H.J Goldsmid, Materials 7, 2577 (2014) (https://doi.org/10.3390/ma7042577).

[11] B.M. Goltsman, B.A. Kudinov, I.A. Smirnov, Semiconductor Thermoelectric Materials Based on Bi_2Te_3 (Nauka, Moskow, 1972).

[12] D. Freik, T. Parashchuk, B. Volochanska, J. Cryst. Growth. 402, 90 (2014) (https://doi.org/10.1016/j.jcrysgro.2014.05.005).

[13] I.V. Horichok, L.I. Nykyruy, T.O. Parashchuk, S.D. Bardashevska, and M.A. Pylyponuk, Mod. Phys. Lett. B 30, 1650172 9 (2016) (https://doi.org/10.1142/S0217984916501724).

[14] G. Chen, M.S. Dresselhaus, J.P. Fleurial, T. Cail lat, Int. Mater. Rev. 48, 45 (2003) (https://doi.org/10.1179/095066003225010182).

[15] M.S. Dresselhaus, G. Chen, M.Y. Tang, R. Yang, L. Hohyun, D. Wang, R. Zhifeng, J.P. Fleurial, and P. Gogna, Adv. Mater. 19, 1043 (2007) (https://doi.org/10.1002/adma.200600527).

[16] Y. Lan, A.J. Minnich, G. Chen, Z. Ren, Adv. Funct. Mater. 20, 357 (2010) (https://doi.org/10.1002/adfm.200901512).

[17] G.S. Nolas, J. Sharp, H.J. Goldsmid, Thermoelectric Basic Principles and New Material Development (Springer, New York, 2001).

[18] G.J. Snyder, E.S. Toberer. Complex thermoelectric materials. Nat. Mater. 7, 105 (2008) (https://doi.org/10.1142/9789814317665_0016).

[19] T. Parashchuk, O. Kostyuk, L. Nykyruy, Z. Dashevsky, J. Mat. Chem. and Phys. 253, 123427 (2020) (https://doi.org/10.1016/j.matchemphys.2020.123427).

[20] N. Bomshtein, G. G. Spiridonov, Z. Dashevsky, Y. Gelbstein, Journal of Electronic Materials 41. 1546 (2012) (https://doi.org/10.1007/s11664-012-1950-8).

[21] T. Parashchuk, Z. Dashevsky, K. Wojciechowski, J. Appl. Phys. 125, 245103 (2019) (doi:10.1063/1.5106422).

[22] K. Wojciechowski, T. Parashchuk, B. Wiendlocha, O. Cherniushok, Z. Dashevsky, J. Mat. Chem. C. 8, 13270 (2020) (https://doi.org/10.1039/D0TC03067H).

O. Kostyuk, B. Dzundza, M. Maksymuk, V. Bublik, L. Chernyak, Z. Dashevsky

[23] J. Jaklovszky, R. Ionescu, N. Nistor, A. Chiculit, Phys Status Solidi 7, 329 (1975) (https://doi.org/10.1002/pssa.2210270202).
[24] Y. Lan Y, B. Poudel, Y. Ma, D. Wang, M.S. Dresselhaus, G. Chen, Z. Ren, Nano Lett. 9, 1419 (2009) (https://doi.org/10.1021/nl803235n).

О. Костюк[1,2], Б. Дзундза[1], М. Максимук[3], В. Бублик[4], Л. Черняк[5], З. Дашевський[6]

Розвиток іскрового плазмового спікання (ІПС) для отримання нанокристалічного термоелектричного матеріалу $Bi_{0.5}Sb_{1.5}Te_3$ p-типу

[1]*Прикарпатський національний університет імені Василя Стефаника, Івано-Франківськ, Україна, bdzundza@gmail.com*
[2]*Івано-Франківський національний медичний університет, Івано-Франківськ, Україна, oksanakostuk@gmail.com*
[3]*Факультет матеріалознавства та кераміки, Університет науки і техніки AGH, Краків, Польща*
[4]*Московський інститут сталі і сплавів Національного університету науки і технологій, Москва, Росія, bublik_vt@rambler.ru*
[5]*Університет Центральної Флориди, США, Leonid.Chernyak@ucf.edu*
[6]*Університет Бен-Гуріона в Негеві, Беер-Шева, Ізраїль, dashevsky.45@mail.ru*

Телурид сурми вісмуту є найбільш часто використовуваним комерційним термоелектричним матеріалом для виробництва електроенергії та охолодження в діапазоні температур 200 - 400 К. Поліпшення експлуатаційних характеристик цих матеріалів доповнюється балансом оптимізації термоелектричних властивостей. Зменшення розміру зерен $Bi_{0,5}Sb_{1,5}Te_3$ суттєво знижує теплопровідність за рахунок розсіювання фононів на границях зерен. У цій роботі показано досягнення іскрового плазмового спікання (ІПС) для отримання нанокристалічних термоелектриків p-типу на основі $Bi_{0,5}Sb_{1,5}Te_3$ при різних температурах (240, 350, 400ºC). Було представлено комплексне дослідження структурних та термоелектричних властивостей $Bi_{0,5}Sb_{1,5}Te_3$. Отримано високе значення безрозмірної термоелектричної добротності $ZT \sim 1$ і навіть трохи більше в діапазоні температур 300 - 400 К для нанокристалічного $Bi_{0,5}Sb_{1,5}Te_3$ p-типу провідності.

Ключові слова: $Bi_{0,5}Sb_{1,5}Te_3$, іскрове плазмове спікання (SPS), термоелектричні властивості.